

## The escape of a particle from a driven harmonic potential to an attractive surface

Z. Tshiprut, J. Klafter, and M. Urbakh<sup>a)</sup>

School of Chemistry, Tel Aviv University, 69978 Tel Aviv, Israel

(Received 22 August 2006; accepted 17 October 2006; published online 27 November 2006)

We investigate theoretically the dynamics of a colloidal particle, trapped by optical tweezers, which gradually approaches an attractive surface with a constant velocity until it escapes the trap and jumps to the surface. We find that the height of the energy barrier in such a colloid-surface system follows the scaling  $\Delta E \propto (z_0(t) - \text{const})^{3/2}$  when the trap approaches the surface,  $z_0(t)$  being the trap surface distance. Using this scaling we derive equations for the probability density function of the jump lengths, for the velocity dependence of its mean and most probable values, and for the variance. These can be used to extract the parameters of the particle-surface interaction from experimental data. © 2006 American Institute of Physics. [DOI: 10.1063/1.2395935]

Thermally activated escape from a trapped state in the presence of a time-evolving barrier plays a central role in diverse systems at the nano- and microscales that at first sight may seem unrelated, but which on closer scrutiny are found to display common features. The latter are shared by numerous systems in physics, chemistry, and biology as exemplified by frictional phenomena at the nanoscale,<sup>1-4</sup> single molecular pulling (unbinding) experiments,<sup>5-8</sup> protein unfolding,<sup>9</sup> cell adhesion and detachment,<sup>10</sup> plastic behavior of glassy materials,<sup>11</sup> and dynamics of colloids at surfaces.<sup>12,13</sup>

In general time-dependent potential barriers can occur either by an external mechanical load or by time-dependent fields. The most frequently used ways to influence the barriers temporally are a slow ramping of a control parameter or a periodic modulation. The rate of the imposed modulation (loading) provides a time scale that can be used to probe and modify the internal dynamics of the system under study. The observed dynamics is determined by the interplay between the rate of thermally assisted escape from the trapped state in the absence of the external perturbation and the external loading rate.

In the present paper we consider the dynamics of a colloidal particle trapped by optical tweezers while approaching an attractive surface until the particle escapes the trap and jumps to the surface. Experimentally, one can measure the probability distribution function (PDF) of the jump lengths for a given approach velocity towards the surface and therefore obtain the velocity dependence of this distribution. Such colloid-surface experiments have been carried out,<sup>12,13</sup> suggesting that they provide information on the particle-surface interaction. It should be noted that the dynamical process studied in these experiments is complementary to the widely discussed single molecular unbinding experiments.<sup>5-9</sup> In the latter case one focuses on a transition from a bound adhesion state to a “free” state located at the minimum of a harmonic potential created by an atomic force microscope or laser

tweezers which are pulled *away* from the adhesion complex. In order to analyze colloid-surface measurements one has to establish relationships between the equilibrium properties of the system and the jump lengths measured under nonequilibrium conditions.

In analogy to the reverse process of unbinding<sup>6</sup> we demonstrate here that in the colloid-surface system the time-dependent height of the barrier follows, to a very good approximation, the scaling relation  $\Delta E \propto (z_0(t) - \text{const})^{3/2}$  when the trap approaches the surface. This scaling is the leading (and dominating) behavior common to driven small-scale systems.<sup>14</sup> Using the scaling relation we derive equations for the PDF of *jump lengths*, for the velocity dependence of its *mean* and *most probable* values, and for the *variance*. These expressions do not include fitting parameters but allow us to extract characteristics of the particle-surface interaction from the experimental data. The analytical equations are in good agreement with the results of numerical simulations using a Langevin equation.

### THE MODEL

The total potential experienced by a particle, trapped by the tweezers, which approaches the surface (see Fig. 1) can be written in the form

$$U(z, t) = U_0(z) + \frac{K}{2}(z - z_0(t))^2. \quad (1)$$

The first term in Eq. (1) describes the particle-surface distance-dependent interaction. Here we assume that this interaction is of van der Waals nature

$$U_0(z) = -\frac{AR}{6z}, \quad (2)$$

where  $A$  is the Hamaker constant,  $R$  is the radius of the particle, and  $z+R$  is the distance between the center of the particle and the surface. The second term in Eq. (1) is the harmonic potential due to the optical trap, which is located at the distance  $z_0(t)+R$  from the surface and has a stiffness  $K$ .

<sup>a)</sup>Electronic mail: urbakh@post.tau.ac.il

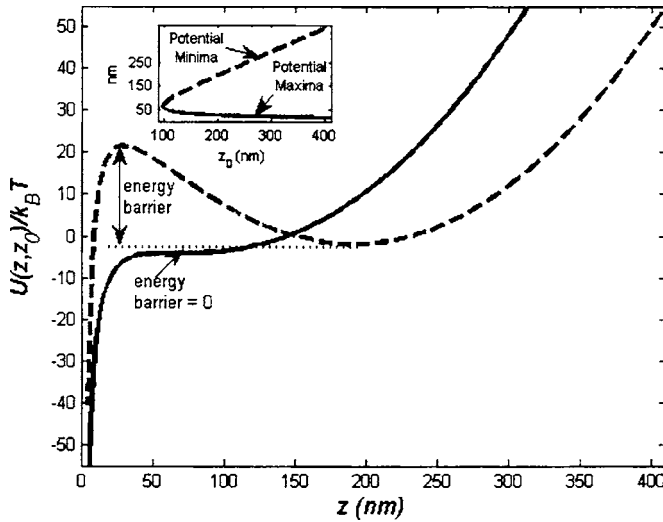


FIG. 1. The interaction potential  $U(z, z_0)$  used in Eq. (1) for two trap-surface separations at two different time instants. The dashed curve corresponds to a large trap-surface separation  $z_0=192$  nm where a pronounced barrier is observed, and the solid curve gives the potential at the critical point  $z_0=z_0^c=98$  nm at which the barrier vanishes. Inset shows the positions of the local minima and maxima of the potential  $U(z, z_0)$  as functions of  $z_0$ . Parameter values:  $A=1.6 \times 10^{-20}$  J,  $R=535$  nm, and  $K=10^{-5}$  N/m.

In the experiments discussed here<sup>12,13</sup> the trap approaches the surface with the constant velocity  $V$  so that

$$z_0(t) = Z_0 - Vt, \quad (3)$$

where  $Z_0$  is the starting position of the trap. The length of the particle jump to the surface is defined as the value of  $z_0$  at the time of the jump.

The dynamical response of the particle can be described by the overdamped Langevin equation

$$\gamma_p \dot{z}(t) = -\frac{\partial U(z, t)}{\partial z} + \xi(t). \quad (4)$$

Here  $\gamma_p$  is the friction coefficient, which, for a spherical particle embedded in a fluid and approaching a surface, can be estimated as<sup>15</sup>

$$\gamma_p = 6\pi R\eta \left(1 + \frac{9}{8} \frac{R}{z+R}\right), \quad (5)$$

where  $\eta$  is a fluid viscosity. The effect of thermal fluctuations is given by a random force, which is  $\delta$ -correlated  $\langle \xi(t)\xi(0) \rangle = 2\gamma_p k_B T \delta(t)$ , where  $k_B$  is the Boltzmann constant and  $T$  is the temperature.

In the *absence* of thermal fluctuations, the particle jumps to the surface when the trap approaches the point  $z_0(t)=z_0^c$ , for which the potential barrier separating the trap and the surface vanishes (see Fig. 1). In this case the jump occurs at the inflection point  $z=z_c$ , where the minimum and the maximum of the potential  $U(z, t)$  merge and

$$\frac{d^2 U(z, t)}{dz^2} = \frac{dU(z, t)}{dz} = 0. \quad (6)$$

For the particle-surface potential given by Eq. (2) the positions  $z_c$  and  $z_0^c$  read

$$z_c = \left(\frac{AR}{3K}\right)^{1/3}, \quad z_0^c = \left(\frac{9AR}{8K}\right)^{1/3}. \quad (7)$$

Using experimentally estimated values<sup>12,13</sup> of  $A=1.6 \times 10^{-20}$  J,  $K=0.01$  pN/nm, and  $R=535$  nm, we get  $z_0^c \approx 100$  nm and  $z_c \approx 65$  nm.

In the presence of fluctuations the jump to the surface may occur for the trap-surface separations which are larger than  $z_0^c$ . Since the thermal fluctuations introduce stochasticity into the problem, we are faced with a distribution of jump lengths. The probability  $W(t)$  that the particle persists in the trap can be approximately calculated through the following kinetic equation:

$$\frac{dW(t)}{dt} = -r(t)W(t), \quad (8)$$

where the time-dependent escape rate  $r(t)$  is given according to Kramers<sup>16</sup> by

$$r(t) = \frac{\omega_1(t)\omega_2(t)}{2\pi\gamma} \exp[-\Delta E(t)/k_B T]. \quad (9)$$

Here  $\Delta E(t)$  is the instantaneous barrier height and  $\omega_{1,2}(t) = \sqrt{|\partial^2 U(z, t)/\partial z^2|}_{z=z_{\mp}}$  are the absolute values of curvatures of  $U(z, t)$  evaluated at the local minimum and maximum of the potential,  $z=z_-$  and  $z=z_+$ , respectively. Using the Kramers equation we assume for simplicity that the friction coefficient  $\gamma_p$  is independent of  $z$  and its value is obtained according to Eq. (5) for  $z=z_c$ .

Equation (9) can be rewritten in terms of the trap position  $z_0(t)$

$$\frac{dW(z_0)}{dz_0} = V^{-1}r(z_0)W(z_0). \quad (10)$$

Then, the experimentally measured PDF for the jump lengths can be written as

$$P(z_0) = \frac{dW(z_0)}{dz_0}. \quad (11)$$

Because of the exponential dependence of the escape rate on  $\Delta E(t)$ , we focus on the behavior of  $r(z_0)$  close to the critical value of the trap position  $z_0(t)=z_0^c$ , for which the barrier disappears completely. In order to evaluate the survival probability  $W(z_0)$  analytically, we expand the combined potential energy  $U(z, z_0)$  around the inflection point  $z=z_c$  to the cubic order [time dependence enters through  $z_0(t)$ ],

$$U \approx U_0(z_c) + \frac{K}{2}(z_0 - z_c)^2 - K(z_0 - z_0^c)(z - z_c) + \frac{U_0'''(z_c)}{6}(z - z_c)^3. \quad (12)$$

The extrema of this truncated potential are given by the expression

$$z_{\pm} = z_c \mp \sqrt{2K(z_0 - z_0^c)/U_0'''(z_c)}. \quad (13)$$

Then, the instantaneous barrier height  $\Delta E = U(z_+, z_0) - U(z_-, z_0)$  and the curvatures  $\omega_{1,2}$  are

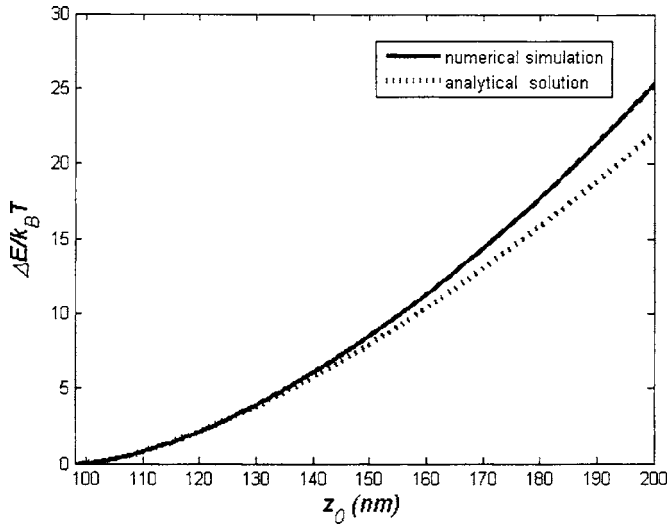


FIG. 2. The height of the potential barrier,  $\Delta E$ , as a function of the trap-surface separation  $z_0$ . The solid curve presents the result of exact calculations according to Eq. (1), and the dashed curve shows the scaling behavior given by Eq. (14). Parameter values are the same as those in Fig. 1.

$$\begin{aligned} \Delta E &= \frac{4\sqrt{2}K^{3/2}}{3(U_0'''(z_c))^{1/2}}(z_0 - z_0^c)^{3/2} \\ &= (2^{5/2}/3^{5/3})(AR)^{1/6}K^{5/6}(z_0 - z_0^c)^{3/2}, \end{aligned} \quad (14)$$

$$\begin{aligned} \omega_{1,2} &= (2KU_0'''(z_c))^{1/4}(z_0 - z_0^c)^{1/4} \\ &= 2^{1/4}3^{1/3}K^{7/12}(AR)^{-1/12}(z_0 - z_0^c)^{1/4}. \end{aligned} \quad (15)$$

Figure 2 shows that the scaling relation (14) accurately describes the  $z_0$  dependence of the barrier height throughout the entire range of the trap-surface separations where the probability of jumps is nonvanishing ( $\Delta E/k_B T < 10$ ).

It should be noted that permissible values of the trap-surface separation  $z_0$  in Eqs. (13)–(15) are limited from below by the value of the critical separation  $z_0^c$  at which the barrier disappears. Equation (9) incorrectly describes the behavior of the preexponential factor at  $z_0 \approx z_0^c$ , predicting that  $r(z_0^c) = 0$  rather than  $r(z_0^c) \gg r(z_0 \gg z_0^c)$ . However, as we will show below, this does not effect an agreement between the results of the analytical approach based on Kramers' theory and the numerical calculations using the Langevin equation (4).

## RESULTS AND DISCUSSION

The solution of the kinetic equation (10) with  $\Delta E$  and  $\omega_{1,2}$  given by Eqs. (14) and (15) leads to the final expression for the PDF  $P(z_0)$ ,

$$\begin{aligned} P(z_0) &= \frac{3V^*}{2V} f(z_0 - z_0^c)^{1/2} \exp\left[-f(z_0 - z_0^c)^{3/2}\right. \\ &\quad \left. - \frac{V^*}{V} \exp[-f(z_0 - z_0^c)^{3/2}]\right], \end{aligned} \quad (16)$$

where

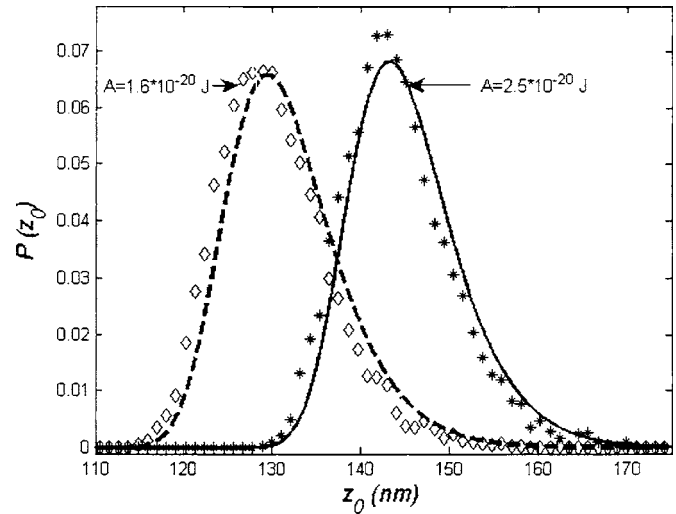


FIG. 3. PDF of the jump lengths calculated for two values of the Hamaker constant,  $A = 1.6 \times 10^{-20}$  J (dashed curve and diamonds) and  $2.5 \times 10^{-20}$  J (solid curve and asterisks). Symbols present results of numerical simulations according to the Langevin equation (4) and curves show analytical prediction given by Eq. (16).  $\eta = 0.01$  P,  $V = 20$  nm/s, and other parameter values similar to those in Fig. 1.

$$f = (2^{5/2}/3^{5/6})K^{5/6}(AR)^{1/6}/k_B T, \quad (17)$$

$$V^* = (3/2)^4(K/(AR))^{1/3}k_B T/(\pi\gamma_p).$$

For the parameters relevant to the experimental conditions<sup>13</sup> we have  $f = 0.0215$  nm<sup>-3/2</sup> and  $V^* = 3458$  nm/s.

Figure 3 shows the agreement between numerical calculations of the PDF for the jump lengths using Langevin Eq. (4) and the analytical form in Eq. (16) which were found for a given driving velocity  $V = 20$  nm/s, and for two values of the Hamaker constant,  $A = 1.6 \times 10^{-20}$  J and  $A = 2.5 \times 10^{-20}$  J. We note the non-Gaussian nature of the distribution and its pronounced asymmetry. We also see that the PDFs are highly sensitive to the value of the Hamaker constant. Thus, fitting the experimental data to Eq. (16), one can determine the parameters of the particle-surface interaction. Equation (16) predicts the dependence of  $P(z_0)$  on experimentally accessible parameters such as the driving velocity, stiffness of the trap, and temperature. Measuring the PDF  $P(z_0)$  for different velocities one can determine not only parameters of the particle-surface potential but also the friction coefficient for the particle approaching the surface. Studies of particle friction coefficients and its dependence on the properties of the solid-fluid interface have attracted a lot of attention recently.<sup>17</sup>

Expression (16) differs essentially from the earlier proposed PDF for the jump lengths which has been derived under the assumption of a linear dependence of the barrier height on the trap position.<sup>13</sup> One can see from Fig. 2 that the linear mapping of the activation energy suggested in Ref. 13 does not work in the relevant range of particle-surface separations. It should also be noted that in contrast to our equation, the PDF in Ref. 13 includes phenomenological parameters which cannot be expressed in terms of the particle-surface interaction potential.

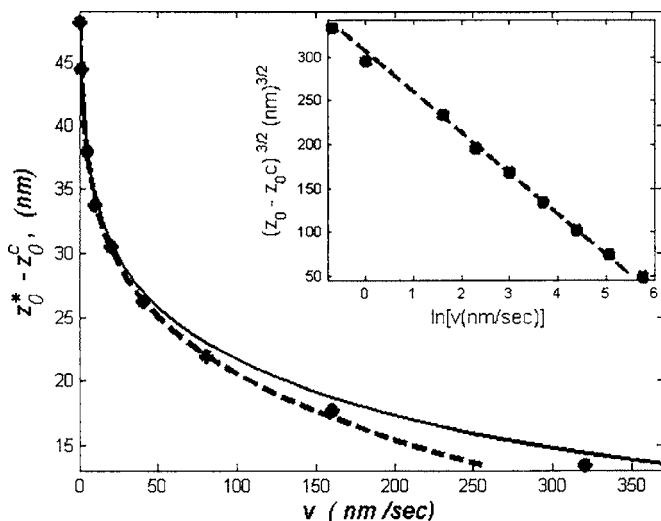


FIG. 4. Variation of the most probable jump length with the pulling velocity  $V$ . Filled circles present results of numerical simulations according to the Langevin equation (4), the solid curve shows analytical results given by Eq. (18), and the dashed curve is the prediction of the scaling relation (19). The inset compares the most probable jump lengths from theory [Eq. (18)] (dashed curve) and simulations (filled circles) in the  $(z_0^* - z_0^c)^{3/2}$  vs  $\ln V$  coordinates.  $\eta = 0.01$  P. Other parameter values the same as those in Fig. 1.

The PDF in Eq. (16) leads to the following equation for the most probable jump length  $z_0^*$  as a function of the driving velocity  $V$

$$V = V^* \frac{f(z_0^* - z_0^c)^{3/2} \exp[-f(z_0^* - z_0^c)^{3/2}]}{f(z_0^* - z_0^c)^{3/2} - 1/3}. \quad (18)$$

In the limit of low driving velocities  $V \ll V^*$ , where  $f(z_0^* - z_0^c)^{3/2} \gg 1/3$ , the above equation reduces to

$$z_0^* = z_0^c + f^{-2/3} \left| \ln \left( \frac{V}{V^*} \right) \right|^{2/3}. \quad (19)$$

The scaling behavior predicted by Eq. (19) is similar to that proposed previously in the context of friction studies using an atomic force microscopy<sup>3,4</sup> (AFM) and of single-molecule unbinding experiments.<sup>6–8</sup> It was demonstrated that for a reliable analysis of these experiments one should invoke a *nonlinear* dependence of the mean frictional and rupture forces on the logarithm of the pulling velocity,  $\langle F \rangle \propto |\ln V|^{2/3}$ . The use of the phenomenological theory<sup>5</sup> assuming the linear logarithmic dependence of the forces on the velocity,  $\langle F \rangle \propto |\ln V|$ , gives parameters of the interaction potentials which can be off by more than an order of magnitude.<sup>8</sup>

In Fig. 4 we compare the analytical results in Eqs. (18) and (19) with the Langevin dynamics simulations. The scaling relation (19) is accurate over a wide range of driving velocities,  $V < 150$  nm/s. It should be noted that the linear logarithmic fit of the phenomenological model<sup>13</sup> is also quite good, but it does not allow us to determine the parameters of the particle-surface interaction from the experimental data.

Using the PDF (16) one can also get the following asymptotic expressions for the mean jump length and variance which are valid for  $V \ll V^*$

$$\langle z_0 \rangle \approx z_0^* + \frac{2}{3} \gamma f^{-2/3} \left| \ln \left( \frac{V}{V^*} \right) \right|^{1/3}, \quad (20)$$

$$\sigma_{z_0}^2 \approx \frac{2\pi^2}{27} f^{-4/3} \left| \ln \left( \frac{V}{V^*} \right) \right|^{-2/3}, \quad (21)$$

where  $\gamma = 0.577 \dots$  is the Euler-Mascheroni constant. Equation (21) predicts a decrease of the variance with a decrease in driving velocity.

In summary, we demonstrated that in a colloid-surface system the height of the energy barrier follows the scaling relation  $\Delta E \propto (z_0(t) - \text{const})^{3/2}$  when the trap approaches the surface. Using the scaling relation we derived equations for the PDF of jump lengths, and the velocity dependence of its mean and most probable values, and the variance. These relations can be used to extract the parameters of the particle-surface interaction from the experimental data. They can also be relevant to the manipulation of single molecules by scanning probes using the “pick-up-and-put-down” approach.<sup>18</sup>

The results obtained here suggest a possible modification of existing force measurements on a single molecule which can be useful to get additional information on the molecular scale energy landscape. Rather than breaking of a bond one has to measure the distribution of the instrument (AFM cantilever or optical tweezers) positions at which the adhesion bond is *created* when the instrument approaches the adhesion complex. Such an experiment can be analyzed using Eqs. (16)–(21). When the trapped state has internal conformations, the driving velocity can determine at which conformation the particle jumps to the adhesion complex.

## ACKNOWLEDGMENTS

J.K. and M.U. acknowledge the support by the German Research Foundation (DFG) via Grant Ha 1517/26-1, 2 (“Single molecules”).

- <sup>1</sup>M. Urbakh, J. Klafter, D. Gourdon, and J. Israelachvili, *Nature (London)* **430**, 525 (2004).
- <sup>2</sup>E. Gnecco, R. Bennewitz, T. Gyalog, Ch. Loppacher, M. Bammerlin, E. Meyer, and H.-J. Güntherodt, *Phys. Rev. Lett.* **84**, 1172 (2000).
- <sup>3</sup>O. Dudko, A. E. Filippov, J. Klafter, and M. Urbakh, *Chem. Phys. Lett.* **352**, 499 (2002).
- <sup>4</sup>S. Sills and R. M. Overney, *Phys. Rev. Lett.* **91**, 095501 (2003).
- <sup>5</sup>E. Evans, *Annu. Rev. Biophys. Biomol. Struct.* **30**, 105 (2001).
- <sup>6</sup>O. K. Dudko, A. E. Filippov, J. Klafter, and M. Urbakh, *Proc. Natl. Acad. Sci. U.S.A.* **100**, 11378 (2003).
- <sup>7</sup>C. L. Dias, M. Dubé, F. A. Oliveira, and M. Grant, *Phys. Rev. E* **72**, 011918 (2005).
- <sup>8</sup>O. K. Dudko, G. Hummer, and A. Szabo, *Phys. Rev. Lett.* **96**, 108101 (2006).
- <sup>9</sup>T. Strunz, K. Oroszlan, R. Schafer, and H.-J. Güntherodt, *Proc. Natl. Acad. Sci. U.S.A.* **96**, 11277 (1999).
- <sup>10</sup>K. Prechtel, A. R. Bausch, V. Marchi-Artzner, M. Kantlehner, H. Kessler, and R. Merkel, *Phys. Rev. Lett.* **89**, 028101 (2002).
- <sup>11</sup>W. L. Johnson and K. Samwer, *Phys. Rev. Lett.* **95**, 195501 (2005).
- <sup>12</sup>P. M. Hansen, J. K. Dreyer, J. Ferkinghoff-Borg, and L. Oddershede,

J. Colloid Interface Sci. **287**, 561 (2005).

<sup>13</sup> J. K. Dreyer, K. Berg-Sørensen, and L. Oddershede, Phys. Rev. E **73**, 051110 (2006).

<sup>14</sup> C. E. Maloney and D. J. Lacks, Phys. Rev. E **73**, 061106 (2006).

<sup>15</sup> J. Happel and H. Brenner, *Low Reynolds Number Hydrodynamics* (Mar-

tinus Nijhoff, The Hague, 1983).

<sup>16</sup> P. Hanggi, P. Talkner, and M. Borkovec, Rev. Mod. Phys. **62**, 251 (1990).

<sup>17</sup> L. Joly, C. Ybert, and L. Bocquet, Phys. Rev. Lett. **96**, 046101 (2006).

<sup>18</sup> O. K. Dudko, A. E. Filippov, J. Klafter, and M. Urbakh, Nano Lett. **3**, 795 (2003).